Numerical schemes for the long-term simulation of SDE's with additive noise and their effectiveness in the integration of a stochastic oscillator

H. de la Cruz[a,*], J. P. Zubelli[a]

[a] *IMPA, Estrada Dona Castorina 110, RJ, Brasil*

Abstract

We propose and analyze numerical methods for the long-term integration of stochastic differential equations (SDEs) with additive noise. By focusing on a linear stochastic oscillator as a test equation, it is shown that these methods are able to reproduce key features related to the long term behavior of this system: they mimic the linear growth of the second moment of the solution, an infinitely-oscillation property and the symplectic structure of this Hamiltonian system. We show the advantages over long periods of time of the proposed integrators in comparison with commonly-used methods for the integration of SDEs. The theoretical findings are illustrated by computer experiments.

Keywords: Stochastic differential equations, numerical methods, linear stochastic oscillator, long-term integration, local linearization method.

1. Introduction

There are many physical applications and practical problems arising in different fields of science and engineering, such as celestial mechanics, quantum physics, biology, finance, neurosciences and statistical physics that require the long term simulation of stochastic differential equations (SDEs). Since in general analytic solutions of these equations are not known or are computationally unfeasible to simulate, efficient numerical schemes capable of preserving as much as possible the key features of the original equation over very long integration intervals are then required.

Numerical integrators commonly used to solve SDEs are traditionally designed over a relative short time interval (cf. [9], [13], [15]). Consequently these integrators may perform poorly for long-time computations and not explain the complete range of behaviour that can be observed in the SDE as the integration time goes to infinity.

In order to investigate the ability of numerical methods to mimic the asymptotic behaviour of SDEs under discretization, one useful idea has been to study the numerical method on a simple test problem whose important traits can be analyzed and which retains key features present in more complex problems of interest. In this spirit two main type of equations have been considered in the literature (see e.g., [5], [7], [9], [11], [15], [16], [17]):

i) the linear equation

$$d\mathbf{X}(t) = \mathbf{A}\mathbf{X}(t)\,dt + dW_t, \qquad t \in \mathbb{R}, \tag{1}$$

where the matrix $\mathbf{A}$ has eigenvalues with negative real part and W is a (two-sided) standard Wiener process; and more recently

ii) the linear stochastic oscillator with additive noise

$$\ddot{\mathbf{X}}(t) + \mathbf{X}(t) = \sigma\dot{W}_t, \qquad \sigma > 0. \tag{2}$$

*Corresponding author

Email addresses: hugo@impa.br (H. de la Cruz), zubelli@impa.br (J. P. Zubelli)

[1]Supported by CNPq under grant no. 500298/2009-2

where W is a standard Wiener process.

The equation (1) has an asymptotically stable solution and from a random dynamical viewpoint it has a random attractor of the flow of solutions, which is determined by its unique stationary solution [1]. Under the consideration that this system can be decoupled, i.e., the matrix $\mathbf{A}$ is diagonalisable, the numerical preservation of these features has been studied by mean of the absolute stability ($A-$stability) property of numerical integrators. It is well known that in general standard explicit integrators do not fulfill the stability assumptions and a large number of implicit methods neither. In [4] a new approach for the construction of $A-$stable explicit integrators was recently proposed.

On the other hand, the stochastic oscillator equation (2) has distinctive long-term properties and also provides a good (simple) model for more general nonlinear stochastic oscillators [10]. This equation can be written as the bidimensional SDE

$$d\mathbf{X}(t) = \mathbf{A}\mathbf{X}(t)\,dt + \mathbf{b}dW_t \tag{3}$$

with

$$\mathbf{A} = \begin{pmatrix} 0 & 1 \\ -1 & 0 \end{pmatrix}, \qquad \mathbf{b} = \begin{pmatrix} 0 \\ \sigma \end{pmatrix}, \qquad \sigma > 0.$$

From the initial point $\mathbf{X}(t_0) = \begin{pmatrix} \mathbf{X}^1(t_0) \\ \mathbf{X}^2(t_0) \end{pmatrix} = \begin{pmatrix} \mathbf{x}_0 \\ \mathbf{y}_0 \end{pmatrix}$ there exists a unique solution over $[t_0, \infty)$ which is given by (see for example [13])

$$\mathbf{X}^1(t) = \mathbf{x}_0 \cos(t) + \mathbf{y}_0 \sin(t) + \sigma \int_{t_0}^{t} \sin(t-s)\,dW_s, \tag{4}$$

$$\mathbf{X}^2(t) = -\mathbf{x}_0 \sin(t) + \mathbf{y}_0 \cos(t) + \sigma \int_{t_0}^{t} \cos(t-s)\,dW_s. \tag{5}$$

This solution has important properties related to the long-term behaviour and symplectic structure. Namely, it satisfies a linear growth property for the second moment [16],

$$\mathbf{P1}) \quad E\left(\|\mathbf{X}(t)\|^2\right) = \mathbf{x}_0 + \mathbf{y}_0 + \sigma^2 (t - t_0)$$

and the oscillatory property [10]

$$\mathbf{P2}) \quad \mathbf{X}^1(t) \text{ has infinitely many zeros, on } [t_0, \infty).$$

On the other hand, since the oscillator (3) is a Hamiltonian system with additive noise, it preserves symplectic structure (cf. [12]). That is, it possess the property

$$\mathbf{P3}) \quad d\mathbf{X}^1(t) \wedge d\mathbf{X}^2(t) = d\mathbf{x}_0 \wedge d\mathbf{y}_0, \qquad \forall t \geq 0.$$

In recent papers, [16], [17], [6], [7], the effect of using different kinds of numerical methods to solve the system (3) have been studied. In parallel, numerical schemes especially devised for approximating this stochastic oscillator were also proposed. In [16] it is shown that the widely used Forward and Backward Euler-Maruyama methods fail to capture the second moment growth rate property **P1**, and from [18] it is also deduced that they do not fulfill the property **P3**. The partitioned Euler-Maruyama method [16] and the Midpoint rule [6], despite inheriting properties **P2**, **P3**, have rates of growth that are not exact and thus the property **P1** is not correctly reproduced. Similar results are obtained in [7] for the Predictor-Corrector methods, where different combinations based on the methods presented in [16] and [6] are studied.

All in all, the proposed methods in the above mentioned references in general do not replicate exactly one or more of the above three properties of (3), the only exception being the EX method, which gives exact reproduction of all these properties. This method is constructed in [17] by rather heuristic considerations.

Even though the EX method behaves very well when integrating the stochastic oscillator, it must be underlined that the complete applicability of this method for more general SDEs could be limited since the computation of the inverses of matrices is required in its numerical implementation.

In this work we propose new numerical methods for the long-term simulation of SDEs with additive noise. Specifically we construct computationally viable integrators that, when applied to (3), result in symplectic methods that reproduce the properties $\mathbf{P1}-\mathbf{P3}$ and are optimal in the sense that they use only increments of the Brownian path in its formulation. Remarkably, we go beyond previous finite-time convergence results by showing that the proposed methods have good mean square error propagation over long time intervals of integration.

The technique presented here to devise these integrators is widely applicable, and we use it to show that the performance of some of the methods reported recently can be notably improved by following the used procedure. We were closely influenced by the papers [3] and [4], where similar ideas were used to construct A-stable higher order numerical integrators for ordinary and stochastic differential equations.

This paper is organized as follows: In Section 2 the ability of some widely-used methods to reproduce properties $\mathbf{P1}-\mathbf{P3}$ is discussed. In Section 3 we present the approach followed for the construction of the integrators proposed in this work. Some particular methods are constructed and their mean-square rate of convergence is studied. In Section 4, general theorems relating the long-term behavior of these methods, when applied to (3), are proved and mean-square error estimates for long time intervals are obtained. Section 5 illustrates the practical performance of these methods through computer experiments. We conclude with some remarks in Section 6.

2. Standard numerical integrators for the stochastic oscillator

For the purpose of completeness and comparison, in this section we review the performance of different commonly-used methods when applied to the stochastic oscillator (3). These methods were studied in [16], [17], [6], [7].

Let $\{t_n\}$, $n=0,1,\ldots$, denote a sequence of equally spaced grid points in time of stepsize h. Results for the long time behavior of the stochastic $\theta-$method [9] when applied to (3) i.e., for the discretization,

$$\mathbf{X}_{n+1}=(\mathbf{I}-\theta h\mathbf{A})^{-1}\left(1+(1-\theta)\,h\mathbf{A}\mathbf{X}_n\right)+(\mathbf{I}-\theta\mathbf{A})^{-1}\,\mathbf{b}\Delta W_n,$$

were reported in [16] for Forward Euler ($\theta=0$), Backward Euler ($\theta=1$) and in [6] for the midpoint rule which coincide with the $\theta-$method (for $\theta=\frac{1}{2}$). Other methods were also proposed and studied in [16], and in [17]. In general when integrating the equation (3), all the resulting iteration maps are given by the recurrence

$$\mathbf{X}_{n+1}=\mathbf{P}\mathbf{X}_n+\mathbf{q}\Delta W_n.$$

The particular expression for $\mathbf{P}$ and $\mathbf{q}$ for these integrators are:

Forward Euler-Maruyama (EM):

$$\mathbf{P}=\begin{pmatrix}1 & h\\ -h & 1\end{pmatrix},\qquad \mathbf{q}=\begin{pmatrix}0\\ \sigma\end{pmatrix}.$$

Backward Euler-Maruyama (BE):

$$\mathbf{P}=\begin{pmatrix}\frac{1}{1+h^2} & \frac{h}{1+h^2}\\ -\frac{h}{1+h^2} & \frac{1}{1+h^2}\end{pmatrix},\qquad \mathbf{q}=\begin{pmatrix}\frac{h}{1+h^2}\sigma\\ \frac{1}{1+h^2}\sigma\end{pmatrix}.$$

Midpoint Rule (MR):

$$\mathbf{P}=\begin{pmatrix}\frac{4-h^2}{4+h^2} & \frac{4h}{4+h^2}\\ -\frac{4h}{4+h^2} & \frac{4-h^2}{4+h^2}\end{pmatrix},\qquad \mathbf{q}=\begin{pmatrix}\frac{2h}{4+h^2}\sigma\\ \frac{4}{4+h^2}\sigma\end{pmatrix}.$$

Partitioned Euler Method (PE):

$$\mathbf{P} = \begin{pmatrix} 1 & h \\ -h & 1-h^2 \end{pmatrix}, \qquad \mathbf{q} = \begin{pmatrix} 0 \\ \sigma \end{pmatrix}.$$

Exponential method (EX):

$$\mathbf{P} = \begin{pmatrix} \cos(h) & \sin(h) \\ -\sin(h) & \cos(h) \end{pmatrix}, \qquad \mathbf{q} = \begin{pmatrix} 0 \\ \sigma \end{pmatrix}.$$

In [7], predictor-corrector methods (named P(EC)^1 methods) were proposed by choosing predictor and corrector integrators from combinations of the different methods above. Specifically the following methods were studied:

P(EC)^1 with PM as predictor and MR as corrector:

$$\mathbf{P} = \begin{pmatrix} 1-\frac{h^2}{2} & h\left(1-\frac{h^2}{2}\right) \\ -h & 1-\frac{h^2}{2} \end{pmatrix}, \qquad \mathbf{q} = \begin{pmatrix} \frac{h}{2}\sigma \\ \sigma \end{pmatrix}.$$

P(EC)^1 with EM as predictor and MR as corrector:

$$\mathbf{P} = \begin{pmatrix} 1-\frac{h^2}{2} & h \\ -h & 1-\frac{h^2}{2} \end{pmatrix}, \qquad \mathbf{q} = \begin{pmatrix} \frac{h}{2}\sigma \\ \sigma \end{pmatrix}.$$

P(EC)^1 with EM as predictor and BE as corrector:

$$\mathbf{P} = \begin{pmatrix} 1-h^2 & h \\ -h & 1-h^2 \end{pmatrix}, \qquad \mathbf{q} = \begin{pmatrix} h\sigma \\ \sigma \end{pmatrix}.$$

P(EC)^1 with MR as predictor and PE as corrector:

$$\mathbf{P} = \begin{pmatrix} 1 & h \\ -h\frac{4-h^2}{4+h^2} & \frac{4-3h^2}{4+h^2} \end{pmatrix}, \qquad \mathbf{q} = \begin{pmatrix} 0 \\ \frac{2-h^2}{2}\sigma \end{pmatrix}.$$

In fact many other P(EC)^1 methods there could arise by applying additional combinations of predictor-corrector methods. In [7] further predictor corrector methods for improving the P(EC)^1 methods were also analyzed.

It is proved that the strong order of convergence of each of the methods above is 1. Let us see their ability to replicate of properties $\mathbf{P1}-\mathbf{P3}$ of the solution to (3).

Concerning the Property **P1** it is proved that the EM produces a second moment with an exponential growth, i.e.,

$$E\left(\|\mathbf{X}_{n+1}\|^2\right) \geq \exp\left(\frac{1}{2}\sigma t_{n+1}\right),$$

and the BE also fails in reproducing the right behavior, showing a second moment bound

$$E\left(\|\mathbf{X}_{n+1}\|^2\right) \leq \mathbf{x}_0 + \mathbf{y}_0 + \frac{\sigma^2}{h}.$$

On the other hand, the other above mentioned methods, although reproducing the linear growth property, do not do it with the required rate. The only exception is the EX method which gives the exact growth $E\left(\|\mathbf{X}_{n+1}\|^2\right) = \mathbf{x}_0 + \mathbf{y}_0 + \sigma^2 t$.

Concerning Property **P2**, with the exception of the P(EC)^1 method (with predictor FE, corrector MR) and the FE, BE (which satisfy a weaker oscillatory property), Property **P2** is correctly reproduced by the rest of the methods. Property **P3** is also peculiar, since most of the methods are not exactly symplectic

when integrating (3). The exception being PE, MR and EX. We must mention here that for the P(EC)[1] methods, this property is approximately preserved, but with certain degree of error.

Summarizing, we can conclude that for the different methods eventually one or more of the properties of the stochastic oscillator is not exactly replicated. Only the EX has a perfect reproduction of all these.

In the next section we formulate the approach that will allow us to construct new integrators with, in general, better properties than the above mentioned methods. We follow [4] for the presentation.

3. Formulation of the approach

Let $(\Omega, \mathcal{F}, P)$ be a complete probability space, and $(\mathcal{F}_t)_{t\geq 0}$ be an increasing right continuous family of complete σ-sub-algebras of $\mathcal{F}$. Consider the d-dimensional SDE with additive noise

$$d\mathbf{X}(t) = \mathbf{f}\left(\mathbf{X}(t)\right) dt + \sum_{j=1}^{m} \mathbf{g}_j\left(t\right) dW_t^j, \qquad t \in [t_0, T], \tag{6}$$

$$\mathbf{X}(t_0) = \mathbf{X}_{t_0}, \tag{7}$$

where W_t^j, $j = 1, \ldots, m$ are $\mathcal{F}_t$-adapted, uncorrelated standard Wiener processes. It is assumed that the $\mathbb{R}^d$-valued measurable functions $\mathbf{f}, \mathbf{g}_j$, satisfy the standard conditions to ensure existence and uniqueness of a strong solution to the problem (6)-(7) [9]. That is, there exists a constant $C > 0$ such that for all $\mathbf{x}_1$, $\mathbf{x}_2$ $\in \mathbb{R}^d$, $t \in [t_0, T]$:

$$\left\|\mathbf{f}\left(\mathbf{x}_1\right) - \mathbf{f}\left(\mathbf{x}_2\right)\right\| \leq C \left\|\mathbf{x}_1 - \mathbf{x}_2\right\|, \tag{8}$$

$$\left\|\mathbf{f}\left(\mathbf{x}_1\right)\right\|^2 \leq C \left(1 + \left\|\mathbf{x}_1\right\|^2\right), \tag{9}$$

Furthermore, let us suppose that $\mathbf{f} \in \mathcal{C}^1\left(\mathbb{R}^d, \mathbb{R}^d\right)$ and denote by $\mathbf{f}_{\mathbf{x}}$ the Jacobian of the function $\mathbf{f}$

Let $(t)_h = \{t_n : n = 0, 1, \ldots, N\}$ be a partition of the time interval $[t_0, T]$, with maximum stepsize h, defined as a sequence of times $t_0 < t_1 < \ldots < t_N = T$ such that $\sup_n (t_{n+1} - t_n) \leq h < 1$ for $n = 0, ..., N-1$. The approach for approximating the solution of (6)-(7) is obtained as follows.

Starting on the initial value $\mathbf{X}_0 = \mathbf{X}_{t_0}$, the approximations $\{\mathbf{X}_i\}$ to $\{\mathbf{X}\left(t_i\right)\}$, $(i = 1, 2, \ldots, N)$ are obtained recursively as follows:

For each time interval of the partition $\mathbf{\Lambda}_n = [t_n, t_{n+1}]$ we consider the stochastic local problem

$$d\mathbf{X}(t) = \mathbf{f}\left(\mathbf{X}(t)\right) dt + \sum_{j=1}^{m} \mathbf{g}_j\left(t\right) dW_t^j, \qquad t \in \Lambda_n, \tag{10}$$

$$\mathbf{X}(t_n) = \mathbf{X}_n,$$

and the associated deterministic local problem

$$d\mathbf{Y}(t) = \mathbf{f}\left(\mathbf{Y}(t)\right) dt, \qquad t \in \Lambda_n, \tag{11}$$

$$\mathbf{Y}(t_n) = \mathbf{X}_n.$$

The solution of (11) can be approximated by one step of the Local Linearization method for ODEs (also known as exponential fitted method) [8]. This is a exponential integrator defined for $t \in \mathbf{\Lambda}_n$ by

$$\mathbf{y}^{LL}\left(t\right) = \mathbf{X}_n + \mathbf{\Phi}(t; t_n, \mathbf{X}_n) \tag{12}$$

with

$$\mathbf{\Phi}(t; t_n, \mathbf{X}_n) = \int_0^{t-t_n} e^{(t-t_n-s)\mathbf{f}_{\mathbf{x}}(\mathbf{X}_n)} \mathbf{f}(\mathbf{X}_n) ds. \tag{13}$$

Let us consider now the stochastic local problem (10). In order to approximate its solution $\mathbf{X}(t)$, we will add a stochastic correction term $\mathbf{R}(t)$ to the LL approximation (12). Thus,

$$\mathbf{X}(t) = \mathbf{y}^{LL}\left(t\right) + \mathbf{R}(t). \tag{14}$$

Since $\mathbf{y}^{LL}(t)$ satisfies the linear equation

$$\begin{aligned} d\mathbf{Y}(t) &= \left(\mathbf{f}_{\mathbf{x}}\left(\mathbf{X}_n\right)\left(\mathbf{Y}(t)-\mathbf{X}_n\right)+\mathbf{f}\left(\mathbf{X}_n\right)\right)dt, \qquad t\in\mathbf{\Lambda}_n, \\ \mathbf{Y}(t_n) &= \mathbf{X}_n, \end{aligned}$$

it is not hard to see that $\mathbf{R}(t)$ satisfies

$$d\mathbf{R}\left(t\right) = \mathbf{q}^{t_n,\mathbf{X}_n}\left(t,\mathbf{R}(t)\right)dt + \sum_{j=1}^{m}\mathbf{g}_j\left(t\right)dW_t^j, \qquad t\in\mathbf{\Lambda}_n, \tag{15}$$

$$\mathbf{R}(t_n) = \mathbf{0}, \tag{16}$$

where

$$\begin{aligned} \mathbf{q}^{t_n,\mathbf{X}_n}\left(t,\mathbf{R}\right) &= \mathbf{f}(\mathbf{y}^{LL}\left(t\right)+\mathbf{R})-\mathbf{f}_{\mathbf{x}}\left(\mathbf{X}_n\right)\left(\mathbf{y}^{LL}\left(t\right)-\mathbf{X}_n\right)-\mathbf{f}\left(\mathbf{X}_n\right) \\ &= \mathbf{f}(\mathbf{X}_n+\mathbf{\Phi}(t;t_n,\mathbf{X}_n)+\mathbf{R})-\mathbf{f}_{\mathbf{x}}\left(\mathbf{X}_n\right)\mathbf{\Phi}(t;t_n,\mathbf{X}_n)-\mathbf{f}\left(\mathbf{X}_n\right). \end{aligned} \tag{17}$$

Thus, by using any existing numerical method for the integration of the SDE (15)-(16), an approximation $\mathbf{Z}_n\left(t\right)$ to $\mathbf{R}\left(t\right)$ in $\mathbf{\Lambda}_n$ is obtained. Then, $\mathbf{X}_{n+1}$ follows from $\mathbf{X}_n$ $(n=0,1,\ldots,N-1)$ by the recursion

$$\mathbf{X}_{n+1} = \mathbf{X}_n + \mathbf{\Phi}(t_{n+1};t_n,\mathbf{X}_n) + \mathbf{Z}_n\left(t_{n+1}\right). \tag{18}$$

It should be noted that an important problem in the evaluation of expression (18) is the efficient evaluation of the integral (13) defining $\mathbf{\Phi}(t;t_n,\mathbf{X}_n)$. This problem was successfully solved in [8] by reducing the evaluation of $\mathbf{\Phi}$ to compute an appropriate matrix exponential. That is,

$$\mathbf{\Phi}(t;t_n,\mathbf{X}_n) = \mathbf{v}_n(t), \tag{19}$$

where $\mathbf{v}_n(t)$ is the $d-$dimensional vector defined by the block matrix identity

$$\begin{bmatrix} \cdots & \mathbf{v}_n(t) \\ 0 & 1 \end{bmatrix} = e^{(t-t_n)\mathbf{C}_n} \tag{20}$$

with

$$\mathbf{C}_n = \begin{bmatrix} \mathbf{f}_{\mathbf{x}}(\mathbf{X}_n) & \mathbf{f}(\mathbf{X}_n) \\ 0 & 0 \end{bmatrix} \in \mathbb{R}^{(d+1)\times(d+1)}.$$

Thus, because of (19), we get the following scheme for the numerical implementation of the method (18):

$$\begin{aligned} \mathbf{X}_{n+1} &= \mathbf{X}_n + \mathbf{v}_n(t_{n+1}) + \mathbf{Z}_n\left(t_{n+1}\right) \\ &= \mathbf{X}_n + [\mathbf{I}_{d-1\times d-1} \quad \mathbf{0}_{d-1\times 1}] \exp\left(\begin{bmatrix} \mathbf{f}_{\mathbf{x}}(\mathbf{X}_n) & \mathbf{f}(\mathbf{X}_n) \\ 0 & 0 \end{bmatrix}(t_{n+1}-t_n)\right)[\mathbf{0}_{1\times d-1} \quad \mathbf{1}]^T + \mathbf{Z}_n\left(t_{n+1}\right). \end{aligned} \tag{21}$$

A number of algorithms may be applied to compute the exponential in (20), See the review in [14]. In particular, those algorithms based on rational (p,q)-Padé approximation ($p\leq q\leq p+2$) combined with the "scaling and squaring" strategy, provide stable approximations to the matrix exponential.

3.1. New numerical integrators

Clearly, from the mechanism described above, a variety of numerical methods can be constructed for solving equation (6)-(7) by applying a one-step numerical integrator to the auxiliary problem (15)-(16). Thus, we could apply any of the methods of Section 2 for devising new integrators.

For instance, when the Forward Euler-Maruyama method is used to integrate the auxiliary equation (15)-(16), it is $\mathbf{q}^{t_n,\mathbf{X}_n}\left(t_n,\mathbf{R}(t_n)\right) = \mathbf{q}^{t_n,\mathbf{X}_n}\left(t_n,\mathbf{0}\right) = \mathbf{0}$, thus the corresponding resulting method is

$$\mathbf{X}_{n+1} = \mathbf{X}_n + \mathbf{\Phi}(t_{n+1};t_n,\mathbf{X}_n) + \sum_{j=1}^{m}\mathbf{g}_j\left(t_n\right)\Delta W_n^j, \tag{22}$$

with $\Delta W_n^j = W_{t_{n+1}}^j - W_{t_n}^j$.

Note that this method is just the exponential scheme (EX) proposed in [17], when the evaluation of $\mathbf{\Phi}$ is done by direct integration of the integral in (13); i.e., by taking $\mathbf{\Phi}(t_{n+1};t_n,\mathbf{X}_n) = (\mathbf{f}_{\mathbf{x}}(\mathbf{X}_n))^{-1}\left(\exp\left(\mathbf{f}_{\mathbf{x}}(\mathbf{X}_n)h\right) - \mathbf{I}\right)\mathbf{f}(\mathbf{X}_n)$ in (22). We point out that for the ill conditioned Jacobian matrix $\mathbf{f}_{\mathbf{x}}(\mathbf{X}_n)$ the EX scheme eventually fails in doing a good integration. In contrast with the scheme (21), where this integral $\mathbf{\Phi}$ is computed with high stability.

Other examples of explicit methods can be obtained by using predictor-corrector methods (P(EC)^1) to integrate (15)-(16). In this way, explicit methods are constructed by taking the (explicit) Euler method as predictor and any $\theta-$method as corrector (e.g., $\theta = 1$ for the Backward Euler method and $\theta = \frac{1}{2}$ for the Trapezoidal method as correctors). Hence the corresponding integrator in this case is:

$$\mathbf{X}_{n+1} = \mathbf{X}_n + \mathbf{\Phi}(t_{n+1};t_n,\mathbf{X}_n) + \theta\left(\mathbf{q}^{t_n,\mathbf{X}_n}\left(t_{n+1},\sum_{j=1}^{m}\mathbf{g}_j\left(t_n\right)\Delta W_n^j\right)\right) + \sum_{j=1}^{m}\mathbf{g}_j\left(t_n\right)\Delta W_n^j. \tag{23}$$

The flexibility of the proposed formulation allows us to select the appropriate method to combine with, in concrete situations.

3.2. Convergence

In this subsection, we study the rate of convergence of the methods (18). To facilitate the exposition, for $\mathbf{y}\in\mathbb{R}^d$ and $s\le t\le\infty$, $\mathbf{X}\left(t;s,\mathbf{y}\right)$ will denote the solution to the original equation (6) at time t which starts from $\mathbf{y}\in\mathbb{R}^d$ at time s. Similarly, $\mathbf{R}\left(t;s,\mathbf{0}\right)$ will denote the solution to the auxiliary equation (15) with initial condition $\mathbf{0}$ at time s. At first, we recall the following theorem concerning the order of strong convergence of numerical methods [11]. For details of the concepts of order of convergence for SDEs see, for example, [9, 11].

Theorem 1 (Milstein [11])**.** *Assume for a one-step discrete time approximation $\mathbf{X}_n$ that the local mean error and the local mean square error satisfy, for all $n = 0,1,\ldots,N-1$, the estimates*

$$\left\|E\left(\mathbf{X}\left(t_{n+1};t_n,\mathbf{X}_n\right) - \mathbf{X}_{n+1}\right)\right\| \le K\left(1+\left\|\mathbf{X}_n\right\|^2\right)^{1/2}h^{\gamma_1}, \tag{24}$$

and

$$\left(E\left(\left\|\mathbf{X}\left(t_{n+1};t_n,\mathbf{X}_n\right) - \mathbf{X}_{n+1}\right\|^2\right)\right)^{1/2} \le K\left(1+\left\|\mathbf{X}_n\right\|^2\right)^{1/2}h^{\gamma_2}, \tag{25}$$

with $\gamma_2 \ge \frac{1}{2}$ and $\gamma_1 \ge \gamma_2 + \frac{1}{2}$. Then

$$\max_{0\le k\le N}\left(E\left\|\mathbf{X}\left(t_k;t_0,\mathbf{X}_{t_0}\right) - \mathbf{X}_k\right\|^2\right)^{1/2} \le C\left(T\right)\left(1+\left\|\mathbf{X}_{t_0}\right\|^2\right)^{1/2}h^{\gamma_2-1/2}$$

where the constant $C\left(T\right)$ depends on the length of the integration interval. That is, the global order of convergence of the discretization $\mathbf{X}_n$ is $\gamma = \gamma_2 - 1/2$.

We note that the various constants throughout the text have been and will be given the same letter K.

Concerning the rate of convergence of the methods (18) we have the following theorem:

Theorem 2. *Let $\mathbf{X}_n$ be the discretization (18) for the SDE (6)-(7) corresponding to some one-step approximation $\mathbf{Z}_n(t)$ to the solution $\mathbf{R}\left(t;t_n,\mathbf{0}\right)$ of the auxiliary equation (15). If the corresponding local mean error (24) and local mean square error (25) of the numerical method $\mathbf{Z}_n(t)$ are such that its global order of convergence is γ. Then, the global order of convergence of $\mathbf{X}_n$ is also γ. That is,*

$$\max_{0\le k\le N}\left(E\left\|\mathbf{X}\left(t_k;t_0,\mathbf{X}_{t_0}\right) - \mathbf{X}_k\right\|^2\right)^{1/2} \le C\left(T\right)\left(1+\left\|\mathbf{X}_{t_0}\right\|^2\right)^{1/2}h^{\gamma}.$$

Proof. The proof is immediate. From (14) and (18) it follows that

$$\mathbf{X}\left(t_{n+1};t_n,\mathbf{X}_n\right)-\mathbf{X}_{n+1}=\mathbf{R}\left(t;t_n,\mathbf{0}\right)-\mathbf{Z}_n(t_{n+1})$$

for each $n=0,1,\ldots,N-1$. Since $\mathbf{Z}_n(t)$ is a one-step approximation of $\mathbf{R}\left(t;t_n,\mathbf{0}\right)$ in $\mathbf{\Lambda}_n$ satisfying the conditions (24)-(25) of Theorem 1, then $\mathbf{X}_n$ also satisfies such conditions. Consequently, the order of converge is the same as $\mathbf{Z}_n$, i.e., γ. □

3.3. The new methods in the integration of the stochastic oscillator

For simplicity of the exposition, in the sequel we consider a uniform partition $(t)_h$ with stepsize h. Applying the numerical time-stepping scheme (21) to the SDE (3), it produces the discrete approximation

$$\mathbf{X}_{n+1}=\mathbf{X}_n+[\mathbf{I}_{d-1\times d-1}\quad\mathbf{0}_{d-1\times 1}]\exp\left(\left[\begin{array}{cc}\mathbf{A}&\mathbf{A}\mathbf{X}_n\\0&0\end{array}\right]h\right)[\mathbf{0}_{1\times d-1}\quad\mathbf{1}]^T)+\mathbf{Z}_n\left(t_{n+1}\right),$$

where, from (17), $\mathbf{Z}_n(t)$ is an approximation to the linear stochastic initial value problem

$$\begin{aligned}&d\mathbf{R}\left(t\right)=\mathbf{A}\mathbf{R}\left(t\right)dt+\mathbf{b}dW_t,\\&\mathbf{R}(t_n)=\mathbf{0}.\end{aligned}\tag{26}$$

The expression

$$\mathbf{v}_n(t_{n+1})=[\mathbf{I}_{d-1xd-1}\quad\mathbf{0}_{d-1x1}]\exp\left(\left[\begin{array}{cc}\mathbf{A}&\mathbf{A}\mathbf{X}_n\\0&0\end{array}\right]h\right)[\mathbf{0}_{1xd-1}\quad\mathbf{1}]^T$$

can be explicitly obtained as follows: since

$$\left[\begin{array}{cc}\mathbf{A}h&\mathbf{A}h\mathbf{X}_n\\0&0\end{array}\right]^k=\left[\begin{array}{cc}(\mathbf{A}h)^k&(\mathbf{A}h)^k\mathbf{X}_n\\0&0\end{array}\right],$$

then

$$\begin{aligned}\mathbf{v}_n(t_{n+1})&=[\mathbf{I}_{d-1\times d-1}\quad\mathbf{0}_{d-1\times 1}]\left(\sum_{k=0}^{\infty}\frac{1}{k!}\left[\begin{array}{cc}\mathbf{A}h&\mathbf{A}h\mathbf{X}_n\\0&0\end{array}\right]^k\right)[\mathbf{0}_{1\times d-1}\quad\mathbf{1}]^T)\\&=\sum_{k=0}^{\infty}\frac{1}{k!}[\mathbf{I}_{d-1\times d-1}\quad\mathbf{0}_{d-1\times 1}]\left[\begin{array}{cc}(\mathbf{A}h)^k&(\mathbf{A}h)^k\mathbf{X}_n\\0&0\end{array}\right][\mathbf{0}_{1\times d-1}\quad\mathbf{1}]^T)\\&=\left(\left(\sum_{k=0}^{\infty}\frac{1}{k!}\left(\mathbf{A}h\right)^k\right)-\mathbf{I}\right)\mathbf{X}_n\\&=\left(\exp\left(\mathbf{A}h\right)-\mathbf{I}\right)\mathbf{X}_n.\end{aligned}$$

Since

$$\mathbf{A}h=\begin{pmatrix}1&i\\i&1\end{pmatrix}\begin{pmatrix}ih&0\\0&-ih\end{pmatrix}\begin{pmatrix}1&i\\i&1\end{pmatrix}^{-1},$$

then

$$\begin{aligned}\exp\left(\mathbf{A}h\right)&=\begin{pmatrix}1&i\\i&1\end{pmatrix}\begin{pmatrix}\exp\left(ih\right)&0\\0&\exp\left(-ih\right)\end{pmatrix}\begin{pmatrix}1&i\\i&1\end{pmatrix}^{-1}\\&=\begin{pmatrix}\cos\left(h\right)&\sin\left(h\right)\\-\sin\left(h\right)&\cos\left(h\right)\end{pmatrix}.\end{aligned}\tag{27}$$

Thus,

$$\mathbf{v}_n(t_{n+1})=\begin{pmatrix}\cos\left(h\right)-1&\sin\left(h\right)\\-\sin\left(h\right)&\cos\left(h\right)-1\end{pmatrix}.$$

Finally, the discrete approximation is

$$\mathbf{X}_{n+1} = \begin{pmatrix} \cos(h) & \sin(h) \\ -\sin(h) & \cos(h) \end{pmatrix} \mathbf{X}_n + \mathbf{Z}_n(t_{n+1}).$$

We are now in conditions to analyze the long time features of the new integrators resulting from approximating the auxiliary equation (15)-(16) by any of the different numerical methods presented in Section 2.

Note that, when applied to the stochastic oscillator, the schemes (21) can be written as

$$\mathbf{X}_{n+1} = \mathbf{M}\mathbf{X}_n + \mathbf{q}\Delta W_n, \tag{28}$$

where

$$\mathbf{M} = \begin{pmatrix} \cos(h) & \sin(h) \\ -\sin(h) & \cos(h) \end{pmatrix},$$

and $\mathbf{q}$ is given for the different methods as in Section 2.

In the next section, the long-time behavior of these methods in the integration of (3) will be studied.

4. Long-time behavior of the proposed integrators

The following theorem deals with second moment behavior of the proposed methods when solving the stochastic oscillator (3). The result shows that the growth property **P1** of the stochastic oscillator is reproduced when applying these methods. Throughout this and the following sections the symbol $(.,.)$ denotes the euclidean scalar product associated to the euclidean vector norm $\|.\|$.

Theorem 3. *The numerical schemes (28), arising from the schemes (21), when applied to the stochastic oscillator (3) with initial condition $\mathbf{X}(t_0) = (\mathbf{x}_0, \mathbf{y}_0)$ satisfies:*

$$E\left(\|\mathbf{X}_{n+1}\|^2\right) = \mathbf{x}_0 + \mathbf{y}_0 + \|\mathbf{q}\|^2 t_{n+1}.$$

Proof. We have

$$E\left(\|\mathbf{X}_{n+1}\|^2\right) = E(\|\mathbf{M}\mathbf{X}_n\|^2 + 2(\mathbf{M}\mathbf{X}_n, \mathbf{R}_n) + \|\mathbf{R}_n\|^2).$$

Since $E(\mathbf{R}_n) = \mathbf{0} \Longrightarrow E(2(\mathbf{M}\mathbf{X}_n, \mathbf{R}_n)) = 0$, we get that

$$\begin{aligned} E\left(\|\mathbf{X}_{n+1}\|^2\right) &= E(\|\mathbf{M}\mathbf{X}_n\|^2 + \|\mathbf{R}_n\|^2) \\ &= E(\|\mathbf{X}_n\|^2) + E(\|\mathbf{R}_n\|^2) \\ &= E(\|\mathbf{X}_n\|^2) + \|\mathbf{q}\|^2 (t_{n+1} - t_0). \end{aligned}$$

Hence, by induction we conclude that

$$E\left(\|\mathbf{X}_{n+1}\|^2\right) = \mathbf{x}_0 + \mathbf{y}_0 + \|\mathbf{q}\|^2 (t_{n+1} - t_0).$$

□

The oscillatory property of the proposed methods is stated in the following theorem:

Theorem 4. *The numerical schemes (28), arising from the schemes (21), when applied to the stochastic oscillator (3) with initial condition $\mathbf{X}(t_0) = (\mathbf{x}_0, \mathbf{y}_0)$ will switch signs infinitely many times as $n \to \infty$, almost surely for all step-time integration.*

Proof. It can be derived from (3) that

$$\begin{aligned}\mathbf{X}_{n+1} &= \mathbf{M}\left(\mathbf{X}_{n-1} + \mathbf{Z}_{n-1}\right) + \mathbf{Z}_n \\ &= \mathbf{M}^2\mathbf{X}_{n-1} + \mathbf{M}\mathbf{Z}_{n-1} + \mathbf{Z}_n \\ &= \dots \qquad (29) \\ &= \mathbf{M}^{n+1}\mathbf{X}_0 + \sum_{k=0}^{n}\mathbf{M}^k\mathbf{Z}_{n-k}. \qquad (30)\end{aligned}$$

From (27),

$$\mathbf{M}^k = \begin{pmatrix} \cos kh & \sin kh \\ -\sin kh & \cos kh \end{pmatrix}.$$

Let $\mathbf{q} = \begin{pmatrix} \mathbf{q}_1 \\ \mathbf{q}_2 \end{pmatrix}$, then

$$\begin{aligned}\mathbf{X}_{n+1}^1 &= \cos\left((n+1)h\right)\mathbf{x}_0 + \sin\left((n+1)h\right)\mathbf{y}_0 + \sum_{k=0}^{n}\left(\mathbf{q}_1\cos kh + \mathbf{q}_2\sin kh\right)\triangle W_{n-k} \\ &= \cos\left((n+1)h\right)\mathbf{x}_0 + \sin\left((n+1)h\right)\mathbf{y}_0 + \sum_{k=0}^{n}V_k,\end{aligned}$$

with $V_k = \left(\mathbf{q}_1\cos kh + \mathbf{q}_2\sin kh\right)\triangle W_{n-k}$. Obviously V_k are independent random variables with distribution $N\left(0,\sigma_k^2\right)$, with $\sigma_k^2 = \left(\mathbf{q}_1\cos kh + \mathbf{q}_2\sin kh\right)^2 h$. Let us compute

$$s_n^2 = \sum_{k=0}^{n}\sigma_k^2.$$

First note that σ_k^2 can be rewritten as

$$\sigma_k^2 = \|\mathbf{q}\|^2\cos^2\left(kh-\alpha\right), \qquad \text{with } \alpha = \arctan\left(\frac{\mathbf{q}_2}{\mathbf{q}_1}\right) \text{ for } \mathbf{q}_1 \neq 0, \text{ and } \alpha = \frac{\pi}{2} \text{ for } \mathbf{q}_1 = 0.$$

Then,

$$\begin{aligned}s_n^2 &= \|\mathbf{q}\|^2 h\sum_{k=0}^{n}\cos^2\left(kh-\alpha\right) \\ &= \left(\frac{\|\mathbf{q}\|^2}{2}\right)h\left(n + \sum_{k=0}^{n}\cos\left(2\left(kh-\alpha\right)\right)\right) \\ &= \left(\frac{\|\mathbf{q}\|^2}{2}\right)h\left(n + \mathrm{Re}\left\{\sum_{k=0}^{n}e^{\mathbf{2}(kh-\alpha)i}\right\}\right) \\ &= \left(\frac{\|\mathbf{q}\|^2}{2}\right)h\left(n + \mathrm{Re}\left\{e^{-\mathbf{2}\alpha i}\sum_{k=0}^{n}e^{\mathbf{2}khi}\right\}\right) \\ &= \left(\frac{\|\mathbf{q}\|^2}{2}\right)h\left(n + \mathrm{Re}\left\{\frac{e^{\mathbf{2}(n+1)hi}-1}{e^{\mathbf{2}(h+\alpha)i}-e^{\mathbf{2}\alpha i}}\right\}\right).\end{aligned}$$

After some algebraic manipulations, we conclude that

$$s_n^2 = \left(\frac{\|\mathbf{q}\|^2}{2}\right)h\left(n + \frac{\sin\left(nh+h\right)\cos\left(nh-2\alpha\right)}{\sin\left(h\right)}\right).$$

Since $\lim_{n\to\infty} s_n^2 = \infty$ and $\sigma_n^2 \leq \|\mathbf{q}\|^2 h$, then

$$\lim_{n\to\infty} \frac{\sigma_n^2}{s_n^2} = 0.$$

It follows from Theorem 1 in [2] that the Law of the Iterated Logarithm may be applied to the sequence $\sum_{k=0}^{n} V_k$. Then,

$$i) \quad P\left(\limsup_{n\to\infty}\left(\frac{\sum_{k=0}^{n} V_k}{\sqrt{2}s_n\left(\log\log s_n\right)^{\frac{1}{2}}}\right) = 1\right) = 1,$$

$$ii) \quad P\left(\liminf_{n\to\infty}\left(\frac{\sum_{k=0}^{n} V_k}{\sqrt{2}s_n\left(\log\log s_n\right)^{\frac{1}{2}}}\right) = -1\right) = 1.$$

From $i)$ for $0 < \varepsilon < 1$,

$$\sum_{k=0}^{n} V_k > (1-\varepsilon)\sqrt{2}s_n\left(\log\log s_n\right)^{\frac{1}{2}} \qquad \text{a.s for infinite values of } n$$

i,e.

$$\mathbf{X}_{n+1}^1 = \cos\left((n+1)h\right)\mathbf{x}_0 + \sin\left((n+1)h\right)\mathbf{y}_0 + \sum_{k=0}^{n} V_k > 0 \qquad \text{a.s, infinitely often.}$$

Similarly from $ii)$ for $0 < \varepsilon < 1$,

$$\sum_{k=0}^{n} V_k < (-1+\varepsilon)\sqrt{2}s_n\left(\log\log s_n\right)^{\frac{1}{2}} \qquad \text{a.s for infinite values of } n$$

i,e.,

$$\mathbf{X}_{n+1}^1 = \cos\left((n+1)h\right)\mathbf{x}_0 + \sin\left((n+1)h\right)\mathbf{y}_0 + \sum_{k=0}^{n} V_k < 0 \qquad \text{a.s, infinitely often.}$$

With this the result follows. □

The theorem below deals with the symplecticity property of the proposed methods:

Theorem 5. *The numerical schemes (28), arising from the schemes (21), when applied to the stochastic oscillator (3) with initial condition* $\mathbf{X}(t_0) = (\mathbf{x}_0, \mathbf{y}_0)$*, preserve the symplecticity structure of this Hamiltonian system. That is,*

$$d\mathbf{X}_{n+1}^1 \wedge d\mathbf{X}_{n+1}^2 = d\mathbf{x}_0 \wedge d\mathbf{y}_0 \qquad \textit{for all } n \in \mathbb{N}.$$

Proof. Let us consider the differential 2-form $d\mathbf{X}_{n+1}^1 \wedge d\mathbf{X}_{n+1}^2$. From (28) it is derived that

$$d\mathbf{X}_{n+1}^1 \wedge d\mathbf{X}_{n+1}^2 = \det(\mathbf{M})\left(d\mathbf{X}_n^1 \wedge d\mathbf{X}_n^2\right).$$

Since $\det(\mathbf{M}) = 1$, the result is obtained immediately. □

As a direct consequence of the above theorems, it can be seen that the proposed methods give better asymptotic integration than widely-used ones. Let us analyze now their error propagation for long time intervals.

4.1. Mean square error propagation for long time intervals

We are going to study the mean-square error estimates of the methods (28) for long time intervals of integration. This analysis is important since standard estimates of the global error of discretization contains factors depending of the length of the integration interval, therefore traditional convergence theory does not work in this scenario of asymptotic integration.

From (4)-(5) we have that the solution $\mathbf{X}(t) = \begin{pmatrix} \mathbf{X}^1(t) \\ \mathbf{X}^2(t) \end{pmatrix}$ of (3) satisfies

$$\mathbf{X}(t_{k+1}) = \mathbf{M}\mathbf{X}(t_k) + \eta_k,$$

with $\mathbf{M}$ as in (28) and

$$\eta_k = \begin{pmatrix} \sigma \int_{t_0}^{t} \sin(t-s)\, dW_s \\ \sigma \int_{t_0}^{t} \cos(t-s)\, dW_s \end{pmatrix}.$$

Hence, we get that

$$\mathbf{X}(t_N) = \mathbf{M}^N \mathbf{X}(t_0) + \mathbf{M}^{N-1}\eta_0 + \ldots + \eta_{N-1}.$$

On the other hand, from (30) we have for our proposed methods that

$$\mathbf{X}_N = \mathbf{M}^N \mathbf{X}_0 + \mathbf{M}^{N-1}\mathbf{q}\Delta W_0 + \ldots + \mathbf{q}\Delta W_{N-1}.$$

Then, the error $e_N = \mathbf{X}(t_N) - \mathbf{X}_N$ in the last point T of the integration interval satisfies:

$$E\|e_N\|^2 = E\left\|\sum_{i=1}^{N} \mathbf{M}^{N-i}(\eta_{i-1} - \mathbf{q}\Delta W_{i-1})\right\|^2 = E\left(\left(\sum_{i=1}^{N} \mathbf{M}^{N-i}(\eta_{i-1} - \mathbf{q}\Delta W_{i-1}), \sum_{i=1}^{N} \mathbf{M}^{N-i}(\eta_{i-1} - \mathbf{q}\Delta W_{i-1})\right)\right)$$

Since $E(\eta_{i-1} - \mathbf{q}\Delta W_{i-1}) = \mathbf{0}$ and because of the random variables $(\eta_{i-1} - \mathbf{q}\Delta W_{i-1})$, $i = 1, 2, \ldots N$ are independent,

$$\begin{aligned} E\|e_N\|^2 &= E\left(\sum_{i=1}^{N} \left(\mathbf{M}^{N-i}(\eta_{i-1} - \mathbf{q}\Delta W_{i-1})\right)^T \left(\mathbf{M}^{N-i}(\eta_{i-1} - \mathbf{q}\Delta W_{i-1})\right)\right) \\ &= E\left(\sum_{i=1}^{N} (\eta_{i-1} - \mathbf{q}\Delta W_{i-1})^T \left(\mathbf{M}^{N-i}\right)^T \mathbf{M}^{N-i}(\eta_{i-1} - \mathbf{q}\Delta W_{i-1})\right). \end{aligned}$$

In addition, as $\left(\mathbf{M}^{N-i}\right)^T \mathbf{M}^{N-i} = \mathbf{I}$, we find that

$$E\|e_N\|^2 = \sum_{i=1}^{N} E\|(\eta_i - \mathbf{q}\Delta W_i)\|^2.$$

For $i = 1, 2, \ldots, N$, we have

$$\begin{aligned} E\|(\eta_i - \mathbf{q}\Delta W_i)\|^2 &= E\left(\|\mathbf{q}\|^2 \Delta W_i^2 + \|\eta_i\|^2 - 2\left(\eta_i^T, \mathbf{q}\Delta W_i\right)\right) \\ &= \left(\|\mathbf{q}\|^2 + \sigma^2\right) h - 4\mathbf{q}_1 \sin^2\left(\frac{h}{2}\right)\sigma - 2\mathbf{q}_2 \sin(h)\,\sigma. \end{aligned}$$

The last equality is obtained from the relations:

$$E\left(\|\mathbf{q}\|^2 \Delta W_i^2\right) = \|\mathbf{q}\|^2 h,$$
$$E\left(\|\eta_i\|^2\right) = h\sigma^2,$$
$$E\left(-2\left(\eta_i^T, \mathbf{q}\Delta W_i\right)\right) = -2\mathbf{q}_1 E\left(\Delta W_i \eta_i^1\right) - 2\mathbf{q}_2 E\left(\Delta W_i \eta_i^2\right) = -4\mathbf{q}_1 \sin^2\left(\frac{h}{2}\right)\sigma - 2\mathbf{q}_2 \sin(h)\,\sigma.$$

Thus,

$$E\|e_N\|^2 = \left(\left(\|\mathbf{q}\|^2 + \sigma^2\right) h - 4\mathbf{q}_1 \sin^2\left(\frac{h}{2}\right)\sigma - 2\mathbf{q}_2 \sin(h)\,\sigma\right) N. \tag{31}$$

Now, we use the result in (31) to compute the mean-square error estimates of the proposed methods:

For the methods constructed by integrating the auxiliary equation (15) by the FE and the PE methods is $\mathbf{q} = \begin{pmatrix} 0 \\ \sigma \end{pmatrix}$. Substituting in (31), it is obtained

$$\begin{aligned} E\|e_N\|^2 &= N\left(2h - 2\sin(h)\right)\sigma^2 \\ &= 2N\left(\frac{h^3}{3!} + O\left(h^5\right)\right)\sigma^2 \\ &= (T - t_0)\left(\frac{2h^2}{3!} + O\left(h^4\right)\right)\sigma^2. \end{aligned}$$

Therefore,

$$\left(E\|e_N\|^2\right)^{\frac{1}{2}} = O\left((T - t_0)^{\frac{1}{2}} h\right).$$

Let us consider now the methods constructed by integrating the auxiliary equation (15) by the BE method. In this case $\mathbf{q} = \begin{pmatrix} \sigma\frac{h}{1+h^2} \\ \sigma\frac{1}{1+h^2} \end{pmatrix}$. From (31) and by algebraic manipulation of trigonometric series, it is obtained that

$$\begin{aligned} E\|e_N\|^2 &= N\left(\frac{h^3 + 2h\cos(h) - 2\sin(h)}{1 + h^2}\right)\sigma^2 \\ &= 2N\left(O\left(\frac{h^3}{1 + h^2}\right)\right)\sigma^2. \end{aligned}$$

Hence,

$$\left(E\|e_N\|^2\right)^{\frac{1}{2}} = O\left((T - t_0)^{\frac{1}{2}} h\right).$$

We can continue in the same way with the rest of the methods. We get the following result:

Proposition 6. *The mean square global error for the schemes (21) in the interval $[t_0, T]$, can be estimated as $O\left((T - t_0)^{\frac{1}{2}} h\right)$. That is, if the length $L = (T - t_0)$ of the integration interval and the stepsize h are such that $L^{\frac{1}{2}} h$ is small, then the global error remain small too.*

Remark 7. *The results above show that the proposed methods have good mean square error propagation over long time intervals $[t_0, T]$, provided that $(T - t_0)^{\frac{1}{2}} h$ is small. In this way the mean square error of commonly-used methods when solving the stochastic oscillator can be improved significantly by following the ideas presented in this paper. In order to exemplify this, let us consider the Euler method. In [12], it is showed that the Euler method has a good error propagation in the interval $[t_0, T_E]$ if $(L_E)^{\frac{3}{2}} h$ is small with $L_E = (T_E - t_0)$. Hence, due to Proposition 6, we can easily conclude that by combining the scheme in (21) with the EM method, the resulting method has a good global error over a larger interval of length $(L_E)^3$. That is, for the same stepsize h, this integrator is applicable on longer times intervals than the Euler method. Numerical experiments in the next section confirm the worth of these results.*

5. Numerical experiments

In this section different numerical experiments are reported. We start by illustrating the practical performance of the proposed methods in solving the stochastic oscillator, corroborating in practice to the theoretical results of the above sections. After this, some numerical tests with nonlinear SDEs are presented. For each one of the methods in Section 2, the corresponding proposed method as defined in (21) will be referred to as LL_"method", where the word to be replaced in the place of "method" depends on the specific integrator used in the construction. For instance, LL_Euler is understood as the integrator (21) obtained by combination with the Euler method. In what follows, we will check the ability of the methods given in (21) to replicate the properties **P1**, **P2**, and **P3** and in each test we will compare our schemes with the conventional standard counterpart. For the sake of comparison, in each figure below, we use the same generated sample path of the Wiener processes in all the involved computations.

5.1. Experiments with the stochastic oscillator

Figure 1 shows a comparison (with respect the second moment evolution of the solution) between the methods LL_BE with BE, LL_P(CE)^1 with P(CE)^1 (with predictor PE, corrector MR), and LL_P(CE)^1 with P(CE)^1 (with predictor EM, corrector MR), when integrating the system (3) with $\sigma = 1$ and initial condition $\mathbf{X}(0) = [1, 0]$ over the time interval $[0, 1000]$. The columns correspond to approximation of $E\|\mathbf{X}(t)\|^2$ obtained with different stepsizes $h_1 = 2^{-3}$, $h_2 = 2^{-2}$, $h_3 = 2^{-1}$. For each scheme 1000 independent realizations of the solution were carried out and $E\|\mathbf{X}_n\|^2$ was calculated by taking the mean of these solutions in the discretization points along these trajectories. For reference a straight line with slope $\sigma^2 = 1$, representing the linear growth of the second moment of the exact solution (Property **P1**) of (3) in $[0, 1000]$, is also plotted in each case. We see that the standard methods fail to reproduce correctly the property **P1** of the exact solution for all the stepsizes. On the contrary, their corresponding LL_standard methods provide a much better reproduction of this long time behavior, even for the larger stepsize $h_3 = 2^{-1}$, so the proposed methods with the LL approach preserve the linear growth property with high accuracy, even for large stepsize and for long time of integration

Figure 2 and 3 concern the oscillatory behavior of the numerical solution of the equation (3). In both cases the parameter was chosen as $\sigma = 0.2$, the initial condition as $\mathbf{X}(0) = [1, 0]$, and the integration interval $[0, 3000]$. Figure 2 shows the trajectories obtained by the MR and the LL_MR method for the stepsizes $h_1 = 2^{-3}$ (first row) and $h_2 = 2^{-2}$ (second row). Figure 3 shows the trajectories obtained by the PE and the LL_PE method with the same stepsizes h_1 and h_2. For comparison purposes, the exact solution (solid line) was also plotted. For a convenient visualization of the trajectories and analysis of the results, in each row, i.e., for each stepsize, we plot the solutions on two subintervals representative of the full integration interval $[0, 3000]$. The results clearly demonstrate that for the standard methods the simulated amplitudes of oscillation are, depending on the interval in consideration, greater or lower than the exact one. In contrast, the LL_MR, and LL_PE methods reproduce the oscillations of system (3) quite accurately. It turns out that the approximate solutions with the LL approach adequately reproduce the right dynamics of the amplitudes of these oscillations.

For the next experiments we consider a numerical test similar to that used in [12]. Figure 4 and 5 present the evolution in the phase plane of system (3) with $\sigma = 1$ and for different initial conditions which are taken over the unit circle with centre at the origin. In Figure 4 the exact solution (which is simulated as indicated in [12]), the solution obtained by the BE, and the solution obtained by the LL_BE method are plotted at three time moments $T_1 = 30$, $T_2 = 50$ and $T_3 = 70$. We have used the stepsize $h = 0.05$. It is known (and can be observed in the figure) that for the linear stochastic oscillator, the exact images of the unit circle are circles with the unit radius shifted from the origin due to the influence of noise. For the numerical methods we are testing, the images also keep this shape, but for the standard BE method the approximation worsens as the time of integration grows. Remarkably, the LL_BE, which by Theorem 5 is a symplectic method, reproduces the exact image much better for every the moment of time.

In Figure 5 we consider even bigger time moments $T_1 = 30$, $T_2 = 70$, $T_3 = 100$ and the numerical integrators to be tested are the P(EC)^1 method (with EM as predictor, BE as corrector) and the symplec-

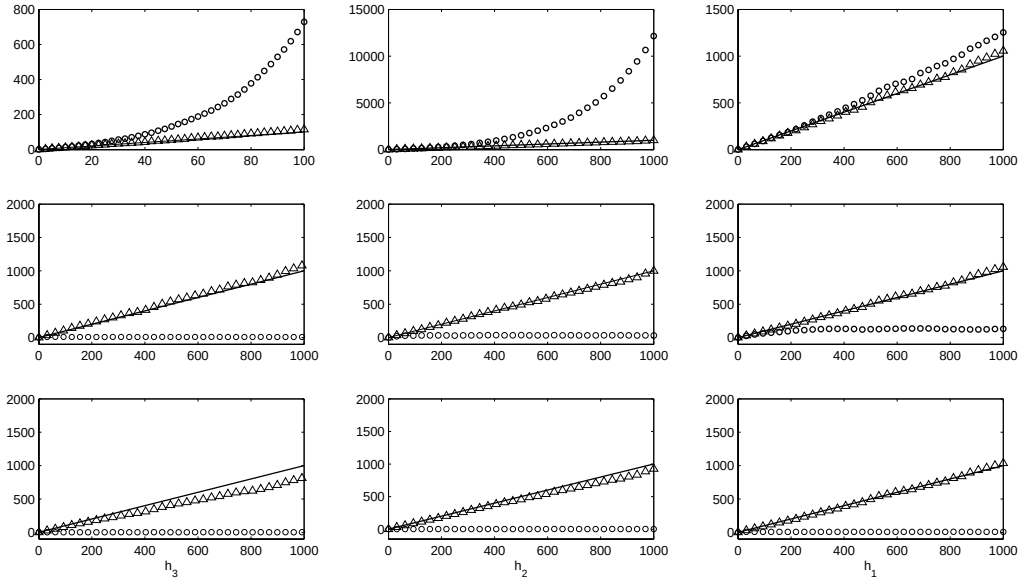

Figure 1: Second moment growth of the numerical approximations of the solution to (3) obtained by standard methods (trajectory of circles) and their LL counterparts (trajectory of triangles) with stepsizes $h_1 = 2^{-3}$, $h_2 = 2^{-2}$ and $h_3 = 2^{-1}$. The lower row shows the performance of the BE and the LL_BE method. The central row shows the methods P(CE)^1 and LL_P(CE)^1 (with predictor PE, corrector MR), and the upper row the methods P(CE)^1 and LL_P(CE)^1 (with predictor EM, corrector MR). For reference the linear growth of the exact solution is represented in each case by a straight line.

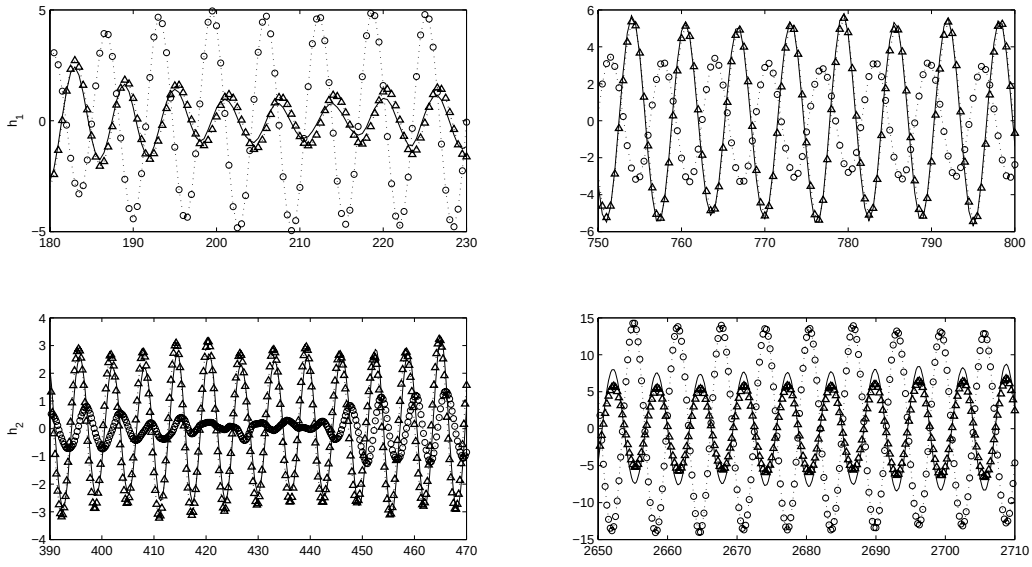

Figure 2: Sample trajectories (in different parts of the integration interval) of the numerical solutions to (3) obtained by the MR method (trajectory of circles) and the LL_MR method (trajectory of triangles) for the stepsizes $h_1 = 2^{-3}$ (first row) and $h_2 = 2^{-2}$ (second row). The trajectory of the exact solution is shown in each case by a solid line.

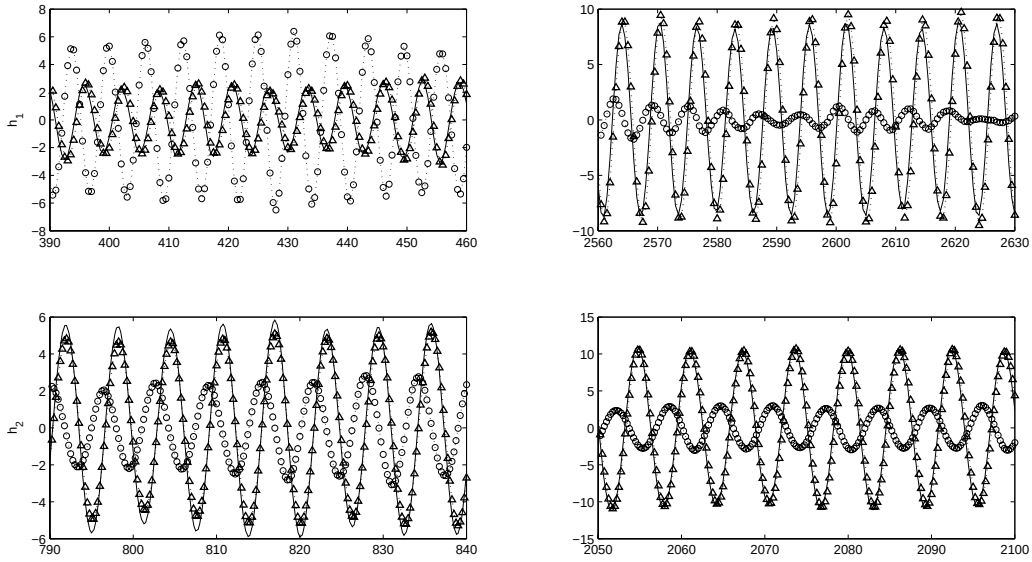

Figure 3: Sample trajectories (in different parts of the integration interval) of the numerical solutions to (3) obtained by the PE method (trajectory of circles) and the LL_PE method (trajectory of triangles) for the stepsizes $h_1 = 2^{-3}$ (first row) and $h_2 = 2^{-2}$ (second row). The trajectory of the exact solution is shown in each case by a solid line.

tic LL_P(EC)^1 method. The results, once again, confirm the effectiveness of proposed methods and the improvement they give over the classical ones.

5.2. Nonlinear examples

The first nonlinear example is the pendulum without damping perturbed by additive noise. This is described by the system

$$\begin{aligned} d\mathbf{X}^1(t) &= \mathbf{X}^2(t)\,dt, \\ d\mathbf{X}^2(t) &= -\sin\left(\mathbf{X}^1(t)\right)dt + \sigma dW_t. \end{aligned} \tag{32}$$

This system was integrated on the interval $0 \le t \le 50$, the initial condition was chosen as $[1.4; 0]$, and the diffusion parameter $\sigma = 1$. Figure 6 shows the trajectories in the phase portrait obtained by a P(EC)^1 method (with predictor the Euler method and corrector the Backward method) as well as the trajectories obtained by the corresponding LLP(EC)^1 method. It is evident that there is no significant difference between the trajectories of these schemes for the smallest stepsize $h = 2^{-11}$, which may be practically regarded as the exact solution for visualization purposes. However this is not the case for larger stepsizes. We observe that for $h = 2^{-2}$ and $h = 2^{-1}$, the numerical solutions of the P(EC)^1 method spiral inwards, showing the wrong qualitative behavior. In contrast, the LLP(EC)^1 method gives a numerical solution that replicates the correct qualitative behavior of the original system.

The next example illustrates the behavior of the proposed methods in the integration of a Lotka-Volterra model with additive noise. Namely

$$\begin{aligned} d\mathbf{X}^1(t) &= \mathbf{X}^1(t)\left(\mathbf{X}^2(t) - 2\right)dt \\ d\mathbf{X}^2(t) &= \mathbf{X}^2(t)\left(1 - \mathbf{X}^1(t)\right)dt + \sigma dW_t. \end{aligned} \tag{33}$$

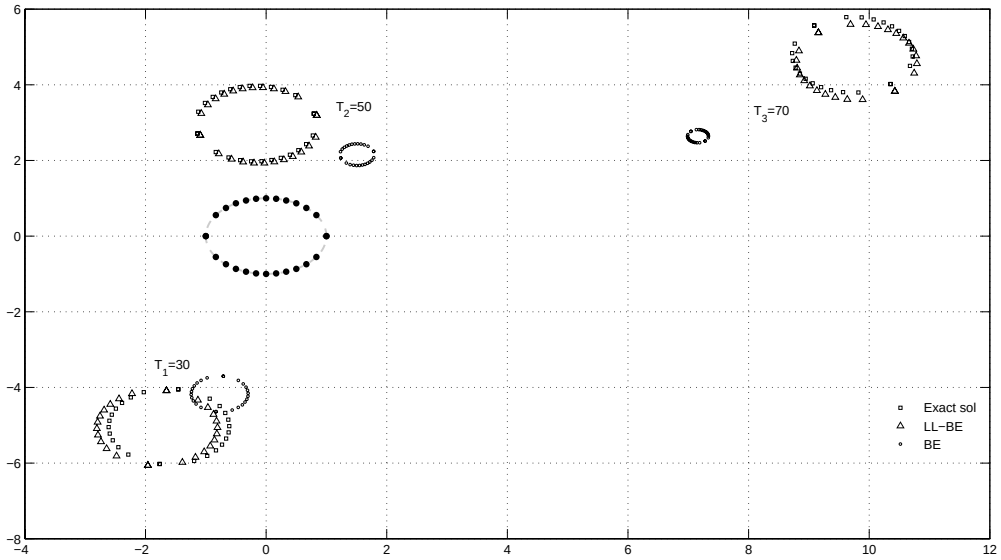

Figure 4: Trajectories in the phase plane of the exact solution and of the numerical approximation to the system (3) obtained by the BM method and the symplectic LL_BM method. The trajectories are obtained from different initial conditions, which are taken over the unit circle centred at the origin, in three moments of time, $T_1 = 30$, $T_2 = 50$ and $T_3 = 70$. The stepsize $h = 0.05$ is used for both integrators.

The effect of the length of the integration interval on the performance of the standard and the proposed integrators is shown in Figure 7. Here, the stepsize is fixed at $h = 0.01$ for the Euler method, and a bigger stepsize $h = 0.2$ is considered for the LLEuler method. The simulations are carried out at three moments of time, $T_1 = 10$, $T_2 = 35$, and $T_3 = 50$ and the initial condition was chosen as $[4; 2]$. As expected, the quality of the numerical approximations get worse as the time of integration increases. For the highest times T_2 and T_3 the standard Euler method results in explosive trajectories (for visualization purposes, in plotting the figure, coordinate axes were conveniently bounded in such a way that explosive behavior is reflected by trajectories reaching the bounding frames).

In contrast, it is observed that the proposed methods (exemplified by the LLEuler) work perfectly, preserving the qualitative behavior of the exact flow (the top row of the figure can be thought of as the actual solution). Even though a higher stepsize $h = 0.2$ was used for the simulations in this case.

6. Concluding Remarks

In this paper we proposed an approach which takes advantage of the suitable compromise between stability and computational reliability of the Local Linearization method to devise numerical schemes for the long-term integration of SDEs. In particular, key asymptotic features of a linear stochastic oscillator can be correctly replicated by the integrators obtained via the ideas presented here.

In most of the previous reported works, only implicit methods behaved well with respect to the long-term integration of the test equation (3). However it is well known that from the view point of efficiency, for general SDEs, implicit methods are inappropriate, since, in general, they involve the numerical solution of a system of nonlinear algebraic equations at each integration step. The situation is even worse when the integration is done over large intervals. One of the advantages of the approach used here, is that it suggests a systematic way of constructing explicit integrators (i.e., that do not require the solution of any algebraic equation) with desirable properties in this respect. For instance the Euler methods, and any $\mathrm{P(EC)}^1$ (with

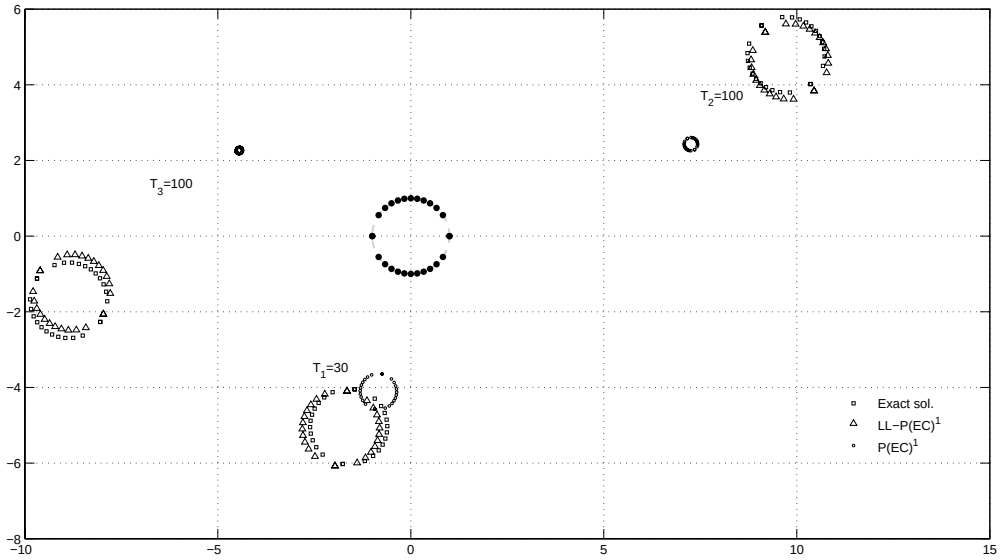

Figure 5: Trajectories in the phase plane of the exact solution and of the numerical approximation to the system (3) obtained by the P(EC)^1 method (with EM as predictor, BE as corrector) and the symplectic LL_P(EC)^1 method. The trajectories are obtained from different initial conditions, which are taken over the unit circle centred at the origin, at three moments of time, $T_1 = 30$, $T_2 = 70$ and $T_3 = 100$. The stepsize $h = 0.05$ is used for both integrators.

an explicit predictor), can be combined as shown in Section 3 to obtain new explicit methods (see e.g., schemes (22) and (23)). The theoretical results in Section 3 and the numerical experiments in Section 5 confirm the superiority of the proposed methods over the corresponding standard ones.

According with the main results of this work and the confirmation of the experimental tests, in our opinion, it makes sense to follow the strategy presented here when the numerical integration of SDEs over long periods of time is required. As we believe, these methods would be useful for many physical applications mainly where integration is required with moderate computational cost. In specific practical situation, the numerical integrator to be chosen among those proposed in this work would depend on the characteristics of the specific problem under consideration.

References

[1] L. Arnold, Random Dynamical Systems, Springer-Verlag, Heidelberg, 1998.

[2] Y.S. Chow and H. Teicher, Probability Theory: Independence, Interchangeability, Martingales., Springer, Berlin, 1978.

[3] H. de la Cruz, R.J. Biscay, F. Carbonell, J.C. Jimenez, and T. Ozaki, Local Linearization-Runge Kutta (LLRK) methods for solving ordinary differential equations, In: Lecture Note in Computer Sciences 3991, Springer-Verlag, (2006), pp. 132-139.

[4] H. de la Cruz, R.J. Biscay, J.C. Jimenez, F. Carbonell, T. Ozaki, High Order Local Linearization methods: an approach for constructing A-stable high order explicit schemes for stochastic differential equations with additive noise, BIT, 50 (2010), pp. 509–539.

[5] D.B. Hernandez, R. Spigler, A-stability of Runge-Kutta methods for systems with additive noise, BIT Numerical Mathematics, 32 (1992), pp. 620-633.

[6] J. Hong, R. Scherer and L. Wang, Midpoint Rule For A Linear Stochastic Oscillator With Additive Noise, Neural, Parallel & Scientific Computations, 14 (2006), pp. 1-12.

[7] J. Hong, R. Scherer and L. Wang, Predictor-Corrector Methods for a Linear Stochastic Oscillator with Additive Noise, Mathematical and Computer Modelling, 46 (2007), pp. 738-764.

[8] J.C. Jimenez, A simple algebraic expression to evaluate the Local Linearization schemes for stochastic differential equations, Appl. Math. Letters, 15 (2002), pp. 775-780.

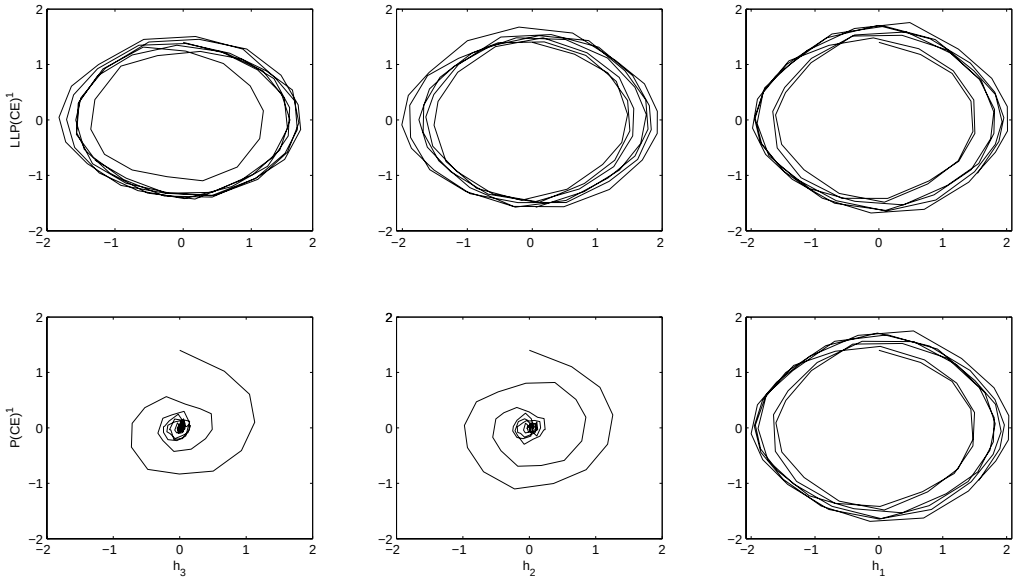

Figure 6: Trajectories in the phase plane obtained from numerical integration of equation (32) with parameter $\sigma = 1$ and different stepsizes $h_1 = 2^{-11}$, $h_2 = 2^{-2}$, $h_3 = 2^{-1}$. The P(EC)^1 method (with Euler as predictor, Backward as corrector) and the LL(EC)^1 integrator were used in this comparison, where approximations computed with the stepsize $h = 2^{-11}$ are thought of as the actual solution.

[9] P.E. Kloeden and E. Platen, Numerical Solution of Stochastic Differential Equations, Springer-Verlag, Berlin, Third Edition, 1999.

[10] L. Markus, A. Weerasinghe, Stochastic oscillators, J. Differential Equations 71 (2) (1988), pp. 288-314.

[11] G.N. Milstein, Numerical Integration of Stochastic Differential Equations, 1995.

[12] G.N. Milstein, Yu.M. Repin and M.V. Tretyakov, Symplectic integration of Hamiltonian systems with additive noise, SIAM J. Numer. Anal. 39 (2002) (6), pp. 2066–2088.

[13] G.N. Milstein , M.V. Tretyakov, Stochastic Numerics for Mathematical Physics, Springer, 2004.

[14] C. Moler and C.F. Van Loan, Nineteen dubious ways to compute the exponential of a matrix, twenty-five years later, SIAM Review, 45 (2003), pp. 3-49.

[15] H. Shurz, Numerical Analysis of Stochastic Differential Equations Without Tears. In: Handbook of Stochastic Analysis and its Applications. Marcel Dekker, Inc: New York, 2002.

[16] A. H. Strømmen and D. J. Higham, Numerical simulation of a linear oscillator with additive noise, Appl. Numer. Math, 51 (2004), pp. 89–99.

[17] A. Tocino, On preserving long-time features of a linear stochastic oscillator, BIT, 47 (2007), pp. 189-196.

[18] A. Tocino, A comparison among several numerical integrators to solve a linear stochastic oscillator, AIP Conference Proceedings, 1048 (2008), pp. 994-998.

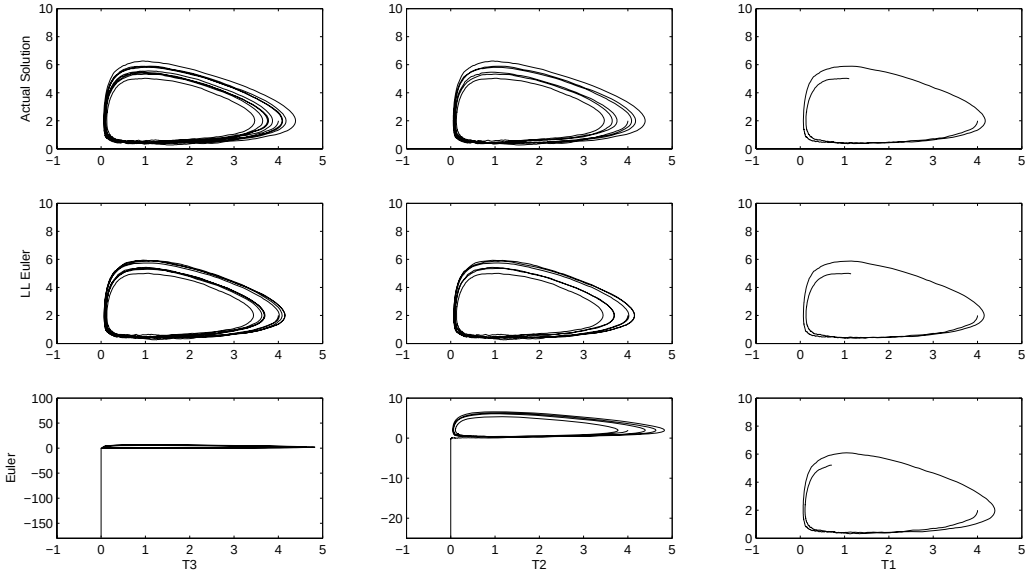

Figure 7: Trajectories in the phase plane obtained from numerical integration of equation (33) at three moments of time, $T_1 = 10$, $T_2 = 35$ and $T_3 = 50$. The Euler method and the corresponding LLEuler method were used in this comparison. The stepsizes $h = 0.01$ and $h = 0.2$ were used by the Euler and the LLEuler integrator respectively. Trajectories in the top row were computed by the Euler method with a very small stepsize $h = 2^{-11}$ and can be thought of as the actual solution.